Global variations in Fourier site response from instrumental observations

Chuanbin Zhu [i)], Brendon A. Bradley [i)], Christopher de la Torre [i)] and Felipe Kuncar [i)]

i) Department of Civil and Natural Resources Engineering, University of Canterbury, Christchurch, New Zealand.

ABSTRACT

Fueled by the advancement in sensor technology and increased seismicity, repeated observations of earthquake-induced ground shakings are accumulated at an unprecedented number of instrumented sites around the globe. Thus, the repeatable (or average) site responses at those recording stations can be disentangled from other systematic effects underlying ground-motion phenomena using regional-network-based approaches, e.g., generalized inversion technique or mixed-effect regression. This provides an excellent opportunity to gain new insights into the global variations in site response, which is impossible via regional studies only. In addition, site response inferred from weak motions based on Fourier amplitude spectrum (FAS), in comparison to that of response spectrum, can maintain the linearity of site response at all frequencies, facilitating a more straightforward physical interpretation. Capitalizing on the high-quality point-observations of Fourier site response in New Zealand, Japan, Europe, and California, we aim to unravel the physical drivers underlying the regional variations in site response, and infer globally consistent patterns, which are essential for developing predictive models transferable across regions. In this preliminary work, we report the global variations in the scaling of Fourier site response with commonly used site characterization parameters/proxies.

Keywords: site response, earthquake, ground motion, variation

1 INTRODUCTION

Earth's near-surface structure (upper few hundreds to kilometers of the crust) significantly modifies the earthquakes waves passing through it. This modification is often referred to as "site effects" (also "site response" or simply "site amplification"), a multitude of frequency-dependent phenomenon. The accurate and precise characterization of site response is crucial to forecast the social and economic impacts of future catastrophic earthquakes.

Due to cheaper sensors and increased seismicity, repeated observations of ground motions are accumulated at an unprecedented number of sites around the globe (Fig. 1). This is particularly the case for seismically active regions with a dense recording network, for instance, Japan (JP), Europe (EU), and California (CA) (e.g., Shible et al., 2023; Shearer et al., 2022). Repeatable (or average) site responses at many individual sites have been disentangled from other systematic effects pertaining to source and propagation path using, for instance, multi-station-based global approaches, e.g., generalized inversion technique (GIT, Andrews 1986; Castro et al. 1990) or mixed-effect residual analysis to ground-motion (prediction) models (GMMs, Abrahamson & Youngs, 1992).

These high-quality point-observations create new opportunities to study the global variations in site response. However, in New Zealand (NZ), such a systematic study on site effects on a national level is lacking. Herein, firstly we thoroughly examine the site-effect phenomena in the entirety of NZ, and then discuss the variations in Fourier site response across NZ, EU, JP, and CA.

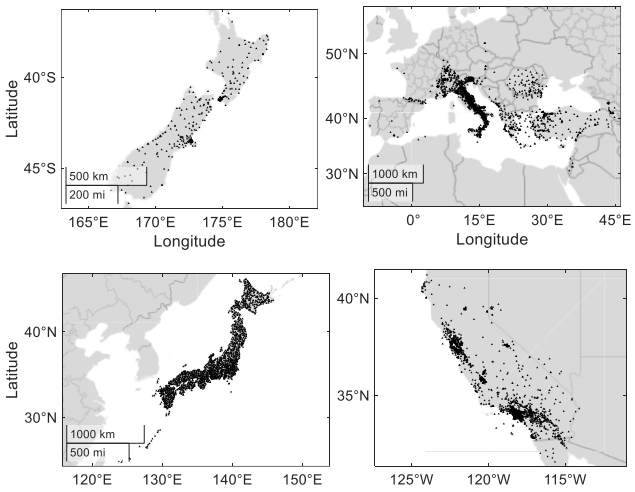

Fig. 1. Dense strong-motion recording networks in NZ, EU, JP and CA.

2 METHODS

2.1 Generalized Inversion Technique (GIT)

For a surface recording during earthquake i at site j, the Fourier amplitude spectrum (FAS) of its horizontal component, $H_{i,j}(f)$, can be represented by the sum of the source $E_i(f)$, path $P_{i,j}(f)$, and site term $S_j(f)$ in natural logarithmic scale (ln):

$$ln\, H_{i,j}(f) = ln\, E_i(f) + ln\, P_{i,j}(f) + ln\, S_j(f). \quad (1)$$

If a regional observation network which recorded multiple events, the above system of linear equations can be solved as a generalized inversion in the least-squares sense (e.g., Andrews, 1986; Castro et al., 1990). Additional constraints are needed to break the trade-offs among the three terms, for instance, on attenuation, assuming $\ln P\left(f, R_{ref}\right) = 0$ where R_{ref} is the reference distance, as well as on site response, assuming no site response at reference site(s).

2.2 Mixed-Effect Regression

In addition to GIT, the other multi-station method to derive site response is the mixed-effect residual analysis (Abrahamson and Youngs, 1992) to predictions from a ground motion model (GMM). If the GMM does not contain any term depicting site effects as a function of site proxy, e.g., V_{S30} (30 m time-averaged shear-wave velocity), then the site term is the full site-response at a given site relative to the mean site response over all stations in the data set (e.g., Kotha et al., 2021). Given the same dataset and constraints, the mixed regression produces identical site responses as GIT (e.g., Bindi et al., 2017).

3 DATA

In NZ and JP, observed site responses are inverted via a nonparametric and semi- parametric GIT in the Fourier space by Zhu et al. (2023) and Nakano et al. (2015), respectively (Fig. 2). Zhu et al. (2023) selected 20,813 ground motions from 1200 crustal events from the acceleration time-histories compiled by Hutchinson et al. (2023) with moment magnitude Mw $\geq$ 3, hypocentral distance $R_{hypo} \leq$ 300 km, and focal depth D $\leq$ 30 km. In JP, Nakano et al. (2015) selected 77,213 strong-ground motions recorded by K-NET, KiK-net and JMA networks from 1996 to 2011 with $M_{JMA} \geq$ 4.5, D $\leq$ 60 km; and $R_{hypo} \leq$ 200 km.

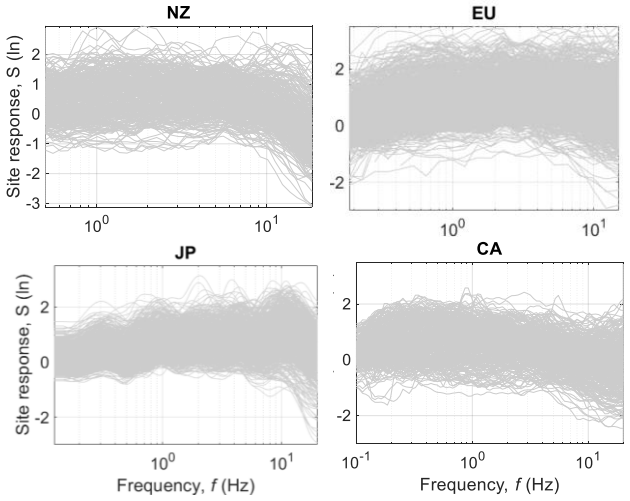

Fig. 2. Fourier site responses at recording sites in different regions.

In EU and CA, site responses were isolated via mixed-effects regression in the Fourier space by Kotha et al. (2021) and Bora et al. (2019), respectively (Fig. 2). Kotha et al. (2021) used records from 3.1$\leq$ Mw $\leq$7.4 and 0< D $\leq$39 km events at distances 0 $\leq R_{JB} <$ 477 km. Bora et al. (2019) selected a subset of NGA-West2 database with M3.2-7.9 earthquakes at distances 0-300 km.

We collect or derive various site data at these instrumented sites with observations. In NZ, we utilize the site database developed by Wotherspoon et al. (2022). However, for information not in the database, e.g., topographic slope (γ, unit: m/m), surface roughness (R_d, unit: m) and relative elevation (H_d, unit: m), we derive them from the NASA's 1-arc-second DEM, NASADEM (NASA JPL, 2021, Data and Resources). *d* is the spatial area surrounding the target pixel. We use three different scales, *d*=80, 370 and 1260 m, respectively, to examine its scale-dependence. For site data in EU, JP, and CA, we retrieve them from databases by Lanzano et al. (2019), Zhu et al. (2021) and Seyhan et al. (2014), respectively.

Histograms of V_{S30} and topographic slope are shown in Fig. 3 and 4, respectively, for each region. Noting that both measured and inferred V_{S30} data are used here to be representative of the geological conditions of all recording sites. Both parameters approximately follow normal distributions in natural logarithmic scale (ln), their probability density functions (PDFs), approximated by standard normal distribution, are also depicted in Fig. 3 and 4 to facilitate comparisons across regions.

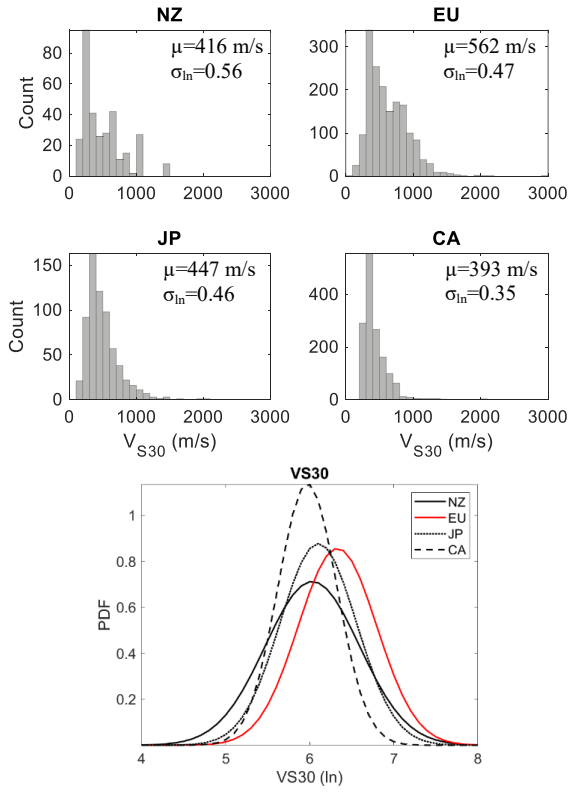

Fig. 3. Histograms of V_{S30} for different regions, and comparison across regions.

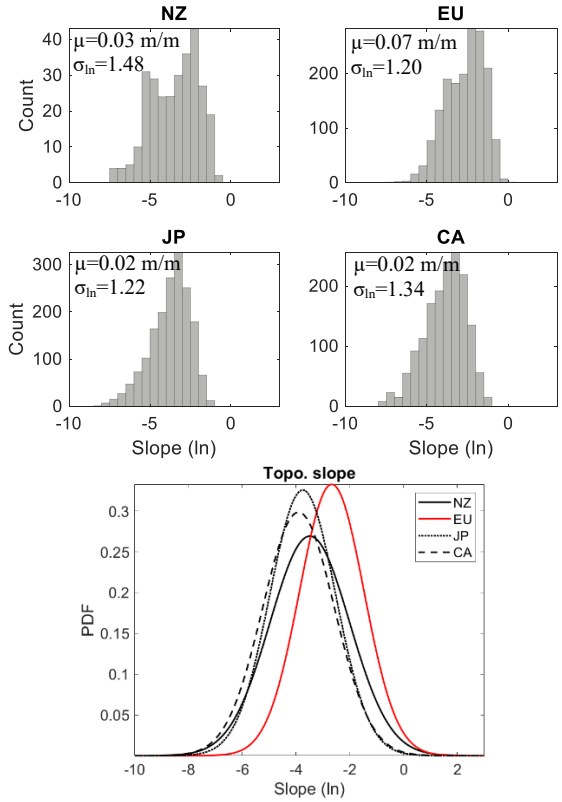

Fig. 4. Histograms of topographic slope γ for different regions, and comparison across regions.

4 OPTIMAL SITE PARAMETERS IN NZ

Site effects are often characterized by discrete variables, e.g., V_{S30}, site period (T_0), depth to a velocity horizon (Z_x, x=0.8, 1.0, and 2.5 km/s), and topographic attributes. Though V_{S30} has been widely used around the globe, the question is whether V_{S30} is the optimal parameter(s) or proxy(s) to parameterize site responses at the frequency range of interest. Answering this question is crucial to both parameter-based classification and regression problems. There exist numerous studies to address this question in other regions (e.g., Bergamo et al., 2021; and many others), but relatively few in NZ (e.g., McVerry, 2011). Herein we seek to tackle this problem and compare the patterns in NZ with those in other regions.

We examine the correlation between Fourier site responses and various site parameters or topographic proxies, as shown in Fig. 5 for f=0.5 Hz. Among the 319 strong-motion sites with observed site response, there are 62, 261 and 75 sites with measured V_{S30}, T_0 and $Z_{1.0}$, respectively. There are no sites with $Z_{2.5}$ measurements. Given the relatively larger sample size for measured T_0, we model the trend between site response and T_0 using a quadratic function, similar to Zhu et al. (2022):

$$\ln Amp(f_p) = \begin{cases} c_1 + c_2 \ln\left(\frac{T_{osc}}{T_0}\right) + c_3 \ln^2\left(\frac{T_{osc}}{T_0}\right) & T_0 < T_{osc} \\ c_1 + c_4 \ln\left(\frac{T_{osc}}{T_0}\right) + c_5 \ln^2\left(\frac{T_{osc}}{T_0}\right) & T_0 \geq T_{osc} \end{cases} \quad (2)$$

where c_1~c_5 are frequency-dependent model coefficients and are solved in regressions.

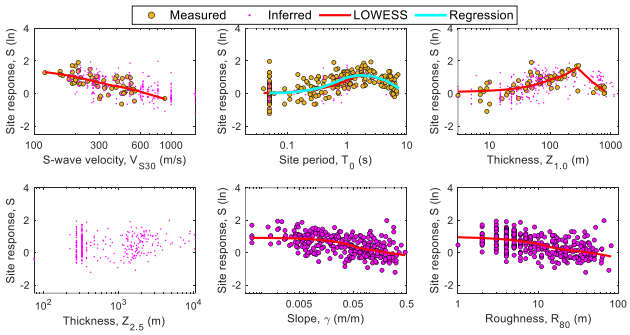

Fig. 5. Fourier site response at f=0.5 Hz vs site parameters/proxies in NZ. Red lines represent the non-parametric locally weighted linear regression (LOWESS) to measured data. Cyan line is the nonlinear least-squares fit (Eq. 2).

Fig. 6 depicts the Pearson product–moment correlations between Fourier site response and measured site parameters in NZ. Noting that, throughout the paper, we interpret the strength of association between two variables using Pearson's R according to the scheme proposed by Schober et al. (2018), i.e., R=0.00-0.10: "negligible"; 0.10-0.39: "weak"; 0.40–0.69: "moderate"; 0.70–0.89: "strong"; 0.90–1.00: "very strong", though there are other interpretations. V_{S30} shows a remarkably strong (Pearson product–moment) correlation (R=~0.7) with site responses for f<2.5 Hz, and a moderate correlation (R=0.40–0.69) for f<4.5 Hz in NZ. In the frequency range from 0.5 to ~8.0 Hz, V_{S30} exhibits the strongest correlation among the measured site parameters, i.e., V_{S30}, T_0 and $Z_{1.0}$. This is different from Japan (e.g., Zhu et al., 2020) and the Central and Eastern North America (CENA) (e.g., Hassani and Atkinson, 2018) where T_0 proves to be the optimal single parameter. This suggests plies that resonance at the examined NZ sites is not as prominent as in Japan and CENA, giving rise to the better performance of V_{S30} than T_0.

In practice, we often utilize both measured and inferred site parameters. We also compare (not shown here) the correlations for site parameters either from direct measurements or inferred from topographic/geological attributes in NZ. Though the correlation for V_{S30} is weakened in comparison to that in Fig. 6, V_{S30} remains the most correlated site parameters with site response in the frequency range from 0.5 to ~8.0 Hz, followed by T_0. Therefore, in both cases, V_{S30} is the optimal single site parameter in the low and mid frequency range (<~8.0 Hz) in NZ.

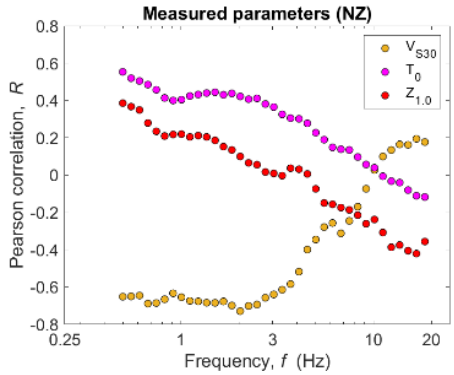

Fig. 6. Pearson's correlation between Fourier site response and measured site parameters in NZ.

Fig. 7 compares the correlations for various topographic proxies in NZ. Slope γ and roughness R_d show moderate correlations with site responses at relatively low frequencies (<~1.0-2.0 Hz), and negligible to weak correlations at higher frequencies. The overall pattern is consistent with those in other regions, e.g., Europe (Bergamo et al., 2021). Besides, in NZ, R_{80}, R_{370} and γ exhibit comparable correlation with site responses in the low frequency range. Regarding the scale-dependence, it has been shown that larger-scale topographic proxies show stronger correlation with site responses at low frequencies than their smaller-scale counterparts, e.g., in Japan and in Europe (Bergamo et al., 2021). However, this does not hold in NZ where smaller-scale R_d tends to perform better. This implies the regional variation in the scaling of topographic proxies with site responses. In addition, we only found a weak to negligible correlation between H_d and site responses in the examined frequency range.

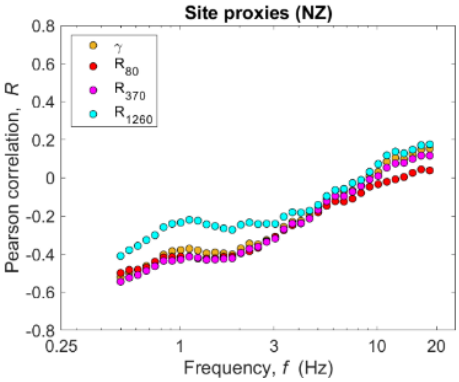

Fig. 7. Pearson's correlation between Fourier site response and topographic proxies in New Zealand. γ – topographic slope, R_d – surface roughness (d= 80, 370, and 1280 m).

5 GLOBAL VARIATIONS IN SITE RESPONSE

Capitalizing on the high-quality point-observations of site response in many regions, in the following we discuss the global variations in Fourier site response and in its scaling with commonly used site characterization parameter/proxy. The advantage of Fourier over response-spectra-based site response is that the former can better capture the high-frequency variability (e.g., Bindi et al., 2017; Zhu et al., 2022).

5.1 Variations in V_{S30}-Amplification Correlation

Fig. 8 compares the strength of V_{S30} (measured) scaling with Fourier site response in NZ, Japan, Europe, and California. It shows that, though there is a consistent trend, the strength of association varies across regions, which is also reported for response-spectra-based site response (e.g., Parker and Stewart, 2021). Though we limit our analysis to measured V_{S30}, we cannot completely rule out the potential impact of different data qualities across regions. However, the regional dependence in V_{S30} scaling is not surprising given the known regional variations in surface geological environments and histories, and thus the dominant physics governing site effects. The complex site effects cannot be fully described by any single parameter. Thus, calibration is often required to a V_{S30}-based model developed for a data-rich region in cross-domain applications.

5.2 Variations in Slope-Amplification Correlation

At localities without V_{S30} measurements, V_{S30} is often first estimated from easy-to-obtain topographic proxies, e.g., slope, geology, or their combination (e.g., Wald and Allen, 2007), and then is utilized to map site response. However, we should keep in mind that the ultimate purpose of such proxy-to-V_{S30} conversion in seismic hazard/risk assessment is to estimate site response. Using sites in Japan, Weatherill et al. (2020) explored an end-to-end approach in which site proxies (e.g., slope) were utilized directly to map site response, rather than via the intermediary, i.e., V_{S30}.

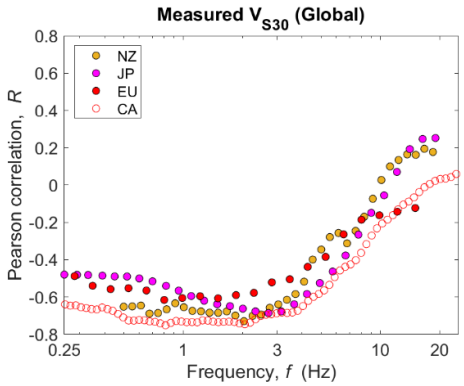

Fig. 8. Comparison of amplification-V_{S30} (measured) correlations across regions.

Capitalizing on the global data set, we examine how the inferred V_{S30} from slope, $V_{S30}(\gamma)$, compares with the direct use of slope, γ, in modelling site response in different regions. Fig. 9 compares the correlations of γ and $V_{S30}(\gamma)$ with Fourier site response in different regions. Noting that γ and $V_{S30}(\gamma)$ data are directly

collected from the NGA-West2 site database (Seyhan et al., 2013) for which 30-arc-sec DEM (different from the background DEM for Fig. 4) was utilized to be compatible with the Wald and Allen (2007)'s V_{S30}-γ model.

We focus on the relatively low frequencies to which site proxies are known to be effective (Fig. 9). In NZ, γ clearly outperforms $V_{S30}(\gamma)$, and there is no discernible difference in Europe and California. However, $V_{S30}(\gamma)$ does show a higher correlation than γ in Japan. Our results in Japan and Europe are consistent with those of Weatherill et al. (2020). They also show that the advantage of $V_{S30}(\gamma)$ over γ diminishes even in Japan when surface geology is also considered. Our results (Fig. 9) lend support for an end-to-end approach in amplification mapping on a regional scale in NZ.

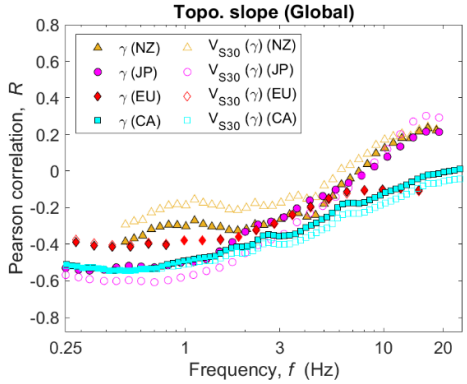

Fig. 9. Comparison of amplification-γ, and amplification-$V_{S30}(\gamma)$ correlations across regions. $V_{S30}(\gamma)$ - V_{S30} estimated from γ using the Wald and Allen (2007) approach. Note that γ and $V_{S30}(\gamma)$ data are directly collected from the NGA-West2 site database for which 30-arc-sec DEM is utilized.

It may be required to further quantify the benefits of this end-to-end approach over the classical method (Wald and Allen, 2007). Future studies could take advantage of localities with observed amplifications by coupling the end-to-end philosophy with geostatistical techniques, e.g., empirical Bayesian regression kriging, in high-resolution amplification mapping which is important for urban disaster risk management and civil protections (ShakeMap, Worden and Wald, 2016; PAGER; Wald et al., 2010).

5.3 Between-Site Variability in Site Response

The between-site (site-to-site or inter-site) variability (ϕ_{S2S}^0 in Zhu et al., 2022) denotes the inherent spatial variability in site response. ϕ_{S2S}^0 is computed as the standard deviation of the (average) site response across sites, and thus depends on the spatial coverage of the sample sites and the complexity of geological conditions in that region. Fig. 10 compares ϕ_{S2S}^0 for the four regions. Noting that ϕ_{S2S}^0 is obtained from Fourier site responses at sites with at least five records to average out the azimuth-dependent effects.

Though ϕ_{S2S}^0 varies across regions, it shows a consistent trend with frequency (Fig. 10). ϕ_{S2S}^0 is approximately within ~0.5-0.7 (ln) in the relatively low and intermediate frequency range where impedance, resonance, and surface and subsurface topographic effects dominate. However, ϕ_{S2S}^0 exhibits a rapid increase for $f > \sim 8$ Hz. At such high frequencies, it is known that attenuation effects (both intrinsic and scattering) become the major site-effect phenomenon. Hence, in addition to the spatial variability in the very near-surface material properties, the between-site variability in deep structures significantly contributes to the increase in ϕ_{S2S}^0 at $f > \sim 8$ Hz. This renders the accurate and precise physics-based simulation of the high-frequency components of ground motions challenging since one would need accurate models in both large and small scales.

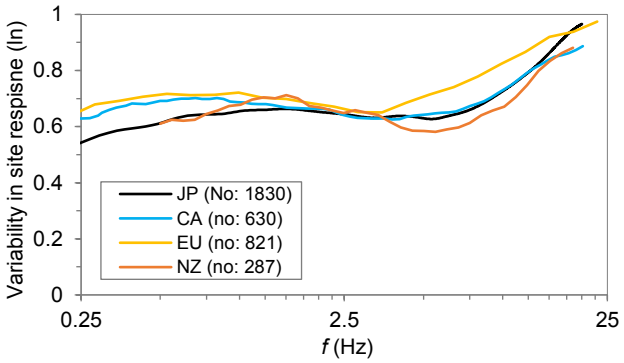

Fig. 10. Between-site variability in Fourier site response in different regions. Only sites with at least five records are utilized in each region.

5 SUMMARIES

Capitalizing on the high-quality point-observations of Fourier site response in New Zealand (NZ), Japan (JP), Europe (EU), and California (CA), we examine the global variations in Fourier site response. V_{S30} is the optimal single site parameter at frequencies lower than <~8.0 Hz in NZ. However, due to different geological environments/histories, the strength of correlation of Fourier site response with V_{S30}, as well as with topographic slope γ, varies across regions.

By comparing the performance of γ with V_{S30} inferred from slope, i.e., $V_{S30}(\gamma)$, the former clearly outperforms the latter in NZ, and there is no discernible difference between the two in EU and CA, and only in JP does $V_{S30}(\gamma)$ show a higher correlation than γ with site response. Our findings support the direct use of γ, namely an end-to-end approach in site-response modelling at sites without V_{S30} measurements in NZ, EU and CA. This end-to-end approach, coupled with empirical Bayesian kriging regression, can be explored in regional site-response mapping.

Another future line of study is on model transferability. Important questions include what constitutes a transferable model, whether a

model/method explicitly capturing more underlying physics (i.e., more site-specific) would be less region dependent and more transferable, and whether a complex foreign model outperforms a simple local model. Addressing these questions has obvious practical implications regarding empirical model development and selection.

It is worth noting that the site responses in our study are relative to the reference conditions in each corresponding region, rather than to a common reference. However, the results of correlation analyses and the between-site variability are insensitive to the reference site conditions.

DATA AND RESOURCES

NASA JPL. NASADEM Merged DEM Global 1 arc second V001. 2020, distributed by NASA EOSDIS Land Processes DAAC, https://doi.org/10.5069/G93T9FD9 (last accessed on 2023-05-05). Topographic attributes were computed using Esri ArcGIS Pro (www.esri.com/software/arcgis).

REFERENCES

1) Abrahamson, N. A. and R. R. Youngs (1992). A stable algorithm for regression analyses using the random effects model. *Bull. Seismol. Soc. Am.* 82, 505-510.
2) Allen, T. I., and D. J.Wald (2007). Topographic slope as a proxy for seismic site-conditions (VS30) and amplification around the globe, U.S. Geol. Surv. Open-File Rept. 2007-1357, 69 pp.
3) Andrews D. J. (1986). Objective determination of source parameters and similarity of earthquakes of different size, in Earthquake Source Mechanics, Das S. Boatwright J., and Scholz C. H. (Editors), Geophysical Monograph Series, Vol. 37, American Geophysical Union, Washington, D.C., 259–267.
4) Bergamo, P., Hammer, C., Fäh, D. (2020). On the Relation between Empirical Amplification and Proxies Measured at Swiss and Japanese Stations: Systematic Regression Analysis and Neural Network Prediction of Amplification. *Bull. Seismol. Soc. Am.* 111, 101–120.
5) Bindi, D., Spallarossa, D. & Pacor, F. (2017). Between-event and between-station variability observed in the Fourier and response spectra domains: comparison with seismological models. *Geophys. J. Int.* 210, 1092–1104.
6) Bora, S.S., Cotton, F., Scherbaum, F. et al. (2017). Stochastic source, path and site attenuation parameters and associated variabilities for shallow crustal European earthquakes. *Bull Earthquake Eng* 15, 4531–4561.
7) Castro, R. R., Anderson, J. G., Singh, S.K. (1990). Site response, attenuation and source spectra of S waves along the Guerrero, Mexico, subduction zone. *Bull. seism. Soc. Am.* 80, 1481–1503.
8) Hassani, B., and G. M. Atkinson (2018). Application of a site-effects model based on peak frequency and average shear-wave velocity to California. *Bull. Seismol. Soc. Am.* 108:351–357.
9) Hutchinson, J. A., C. Zhu, B. A. Bradley, R. L. Lee, L. M. Wotherspoon, M. Dupuis, C. Schill, J. Motha, E. F. Manea, and A. E. Kaiser (2023). 2023 New Zealand Ground Motion Database. *Bull. seism. Soc. Am.* (under review).
10) Kotha, S.R., Bindi, D., Cotton, F. (2022). A regionally adaptable ground-motion model for fourier amplitude spectra of shallow crustal earthquakes in Europe. *Bull Earthquake Eng* 20, 711–740.
11) Lanzano , G. , Sgobba, S. & Luzi, L., 2019. The pan-European Engineering Strong Motion (ESM) flatfile: compilation criteria and data statistics, *Bull Earthquake Eng*, 17, 561–582.
12) McVerry GH (2011) Site-efect terms as continuous functions of site period and Vs30. In: Pacifc conference on earthquake engineering: building an earthquake resilient society, Auckland, New Zealand.
13) NASA JPL (2021). NASADEM Merged DEM Global 1 arc second V001. Distributed by OpenTopography. https://doi.org/10.5069/G93T9FD9. Accessed: 2023-05-01
14) Nakano, K., Matsushima, S., Kawase, H. (2015). Statistical Properties of Strong Ground Motions from the Generalized Spectral Inversion of Data Observed by K‐NET, KiK‐net, and the JMA Shindokei Network in Japan. *Bull. Seismol. Soc. Am.* 105, 2662-2680.
15) Parker, G. A., and A. S. Baltay (2022). Empirical Map-Based Nonergodic Models of Site Response in the Greater Los Angeles Area. *Bull. Seismol. Soc. Am.* XX, 1–23, doi: 10.1785/0120210175
16) Schober P, Boer C and Schwarte LA (2018). Correlation coefficients: Appropriate use and interpretation. Anesthesia & Analgesia 126, 1763–1768.
17) Seyhan, E., J. P. Stewart, T. D. Ancheta, R. B. Darragh and R. W. Graves (2014). NGA-West2 Site Database. *Earthq. Spectra* 30, 1007–1024.
18) Shearer, P. M., Abercrombie, R. E., & Trugman, D. T. (2022). Improved stress drop estimates for M 1.5 to 4 earthquakes in southern California from 1996 to 2019. *Journal of Geophysical Research: Solid Earth*, 127, e2022JB024243. https://doi.org/10.1029/2022JB024243.
19) Shible, H., F. Hollender, D. Bindi, P. Traversa, A. Oth, B. Edwards, P. Klin, H. Kawase, I. Grendas, R. R. Castro, et al. (2022). GITEC: A Generalized Inversion Technique Benchmark, *Bull. Seismol. Soc. Am.* XX, 1–28, doi: 10.1785/0120210242.
20) Wald, D. J., K. S. Jaiswal, K. D.Marano, D. B. Bausch, andM. G.Hearne (2010). PAGER—Rapid assessment of an earthquake's impact, U.S. Geol. Surv. Fact Sheet 2010-3036, 4 pp., revised November 2011.
21) Weatherill, G., S. R. Kotha, and F. Cotton (2020). Re-thinking site amplification in regional seismic risk assessment. *Earthq. Spectra* doi.org/10.1177/8755293019899956
22) Wotherspoon LM, Kaiser AE, Manea EF, Stolte AC (2022). National Seismic Hazard Model: Site Characterisation Database summary report. Lower Hutt (NZ): GNS Science. 54 p. (GNS Science report; 2022/28).
23) Worden, C. B., and D. J. Wald (2016). ShakeMap documentation, U.S. Geol. Surv., available at https://usgs.github.io/shakemap/ (last accessed April 2020).
24) Zhu, C., M. Pilz, and F. Cotton (2020). Which is a better proxy, site period or depth to bedrock, in modelling linear site response in addition to the average shear-wave velocity? *Bull. Earthq. Eng.* 18, 797–820.
25) Zhu, C., Weatherill, G., Cotton, F., Pilz, M., Kwak, D. Y., Kawase, H. (2021). An open-source site database of strong-motion stations in Japan: K-NET and KiK-net (v1.0.0). *Earthq. Spectra* 37, 2126-2149.
26) Zhu, C., F. Cotton, H. Kawase, K. Nakano (2022). How Well Can We Predict Earthquake Site Response So Far? Machine Learning vs. Physics-Based Modeling. *Earthquake Spectra*, https://doi.org/10.1177/87552930221116399